

Manifestation of the roughness-square-gradient scattering in surface-corrugated waveguides

F. M. Izrailev*

Instituto de Física, Universidad Autónoma de Puebla, Apartado Postal J-48, Puebla, Pue. 72570, México

N. M. Makarov†

Instituto de Ciencias, Universidad Autónoma de Puebla, Priv. 17 Norte No. 3417, Col. San Miguel Hueyotlipan, Puebla, Pue. 72050, México

M. Rendón‡

Facultad de Ciencias de la Electrónica, Universidad Autónoma de Puebla, Puebla, Pue. 72570, México

(Received 19 October 2005; published 19 April 2006)

We study a mechanism of wave and electron scattering in multimode surface-corrugated waveguides and wires. This mechanism is due to the presence of square-gradient terms in an effective Hamiltonian describing the surface scattering, which were neglected in all previous studies. With a careful analysis of the role of the roughness slopes in a surface profile, we show that these terms can strongly contribute to the expression for the inverse attenuation length L_n (mean free path). Specifically, at any fixed value of a roughness height σ , with a decrease of the correlation length R_c our mechanism begins to predominate over the other, known one. This predominance is due to a quite specific form of the square-gradient power spectrum as a function of R_c and arises in spite of the fact that the corresponding contribution to L_n^{-1} is proportional to $\propto\sigma^4$ in contrast to standard terms proportional to $\propto\sigma^2$. It is remarkable that the square-gradient mechanism prevails in a widely discussed region of small-scale roughness where the corrugated surface is typically described via white noise.

DOI: [10.1103/PhysRevB.73.155421](https://doi.org/10.1103/PhysRevB.73.155421)

PACS number(s): 73.21.Hb, 42.25.Dd

I. INTRODUCTION

The subject of wave transport through guiding surface-disordered systems is of great importance in various physical applications. Recently, this topic has attracted even more attention due to a burst of developments in nanoscience where frequently one deals with devices or structures (quantum wires, leads, etc.) whose surface's irregularities become more important than those in the bulk. Other situations for either electromagnetic or acoustic waves (remote sensing, photonic and acoustic devices, optical thin films, etc.) are analogous. Therefore, in what follows we do not make any distinction between electromagnetic and electron waves or any other type of waves.

In spite of extensive research on wave scattering from rough surfaces, the problem of transport in the waveguides with such profiles still remains open. This problem is a great theoretical challenge since it deals with the multiple scattering of a wave from lateral walls. As a result of this scattering, the unperturbed longitudinal wave number k_n of an n th propagating normal mode changes, $k_n \rightarrow k_n + \delta k_n$, due to a complex amount δk_n ,

$$\delta k_n = \gamma_n + i(2L_n)^{-1}. \quad (1.1)$$

The real part γ_n arises due to a roughness-induced correction to the phase velocity, while L_n is the *total* electron mean free path or *scattering length* of a given mode. In the wave-propagation theory this quantity is usually called the *extinction* or *attenuation length* of a mean field. As is known, the shift γ_n does not change static transport properties of a disordered system. Therefore, our further analysis shall be focused only on the attenuation length L_n .

Evidently, statistical properties of a rough surface profile $\xi(x)$ give a strong impact on the scattering process. However, a proper incorporation of these properties into the theory accounting for the guided and scattered waves is not a trivial task. Many approaches have been proposed in connection with the surface scattering (see, e.g., Refs. 1–18 and references therein). One of the main tools to treat this problem is a reduction of the *surface* scattering to the *bulk* one in such a way that the latter can be formally described by an effective Hamiltonian \hat{H} ,

$$\hat{H}^{(0)} \rightarrow \hat{H} = \hat{H}^{(0)} + \hat{U}, \quad (1.2)$$

with flat boundaries, however, with a complicated potential \hat{U} . To the best of our knowledge, originally the idea of this approach was discussed by Migdal.¹⁹ After, it was frequently used in the theories of classical and quantum wave scattering; see, e.g., Refs. 6–14. One should stress that in the majority of them^{6–11} the study was restricted to the lowest order in the root-mean-square roughness height σ . Specifically, the higher-order terms were omitted in the effective Hamiltonian due to their seeming smallness. Other methods^{12–18} were mainly based on a principal assumption that the surface roughness is sufficiently smooth.

It should be stressed that the above formal reduction of surface scattering to the Hamiltonian with a potential containing random profiles does not mean an equivalence between surface and bulk scattering. The point is that the obtained “bulk” Hamiltonian is of very specific form that does not allow to use standard random matrix approaches based on a complete randomness in effective potentials. Moreover, after numerical results^{4,5} demonstrating the peculiarities of

surface scattering (in particular, the coexistence of ballistic, diffusive, and localized modes) it becomes clear what the principal difficulties are for nonperturbative statistical approaches to the surface scattering.

In this paper we present analytical results demonstrating a scattering mechanism missed in previous studies of the surface scattering. This mechanism is due to specific *square-gradient* terms that are proportional to $\sigma^2 \xi'^2(x)$ in the potential \hat{U} . We argue that the discovered scattering mechanism is substantially different from the known ones associated with the *roughness amplitude* and *roughness gradient* of the surface.

The two last mechanisms have been already studied (see, e.g., Refs. 1, 10, and 11). Their main contributions were shown to depend on the terms containing the quantities $\sigma \xi(x)$ and $\sigma \xi'(x)$, respectively. In the analysis performed the square-gradient terms related to our scattering mechanism were discarded due their seemingly small contribution. Indeed, the square-gradient terms are formally proportional to σ^2 , similar to other terms that arise in the next (second-order) approximation in the amplitude and gradient roughness. However, we have found that the square-gradient terms have a very strong dependence on the roughness correlation length R_c , in contrast with those terms appearing in the second-order approximation. Specifically, with a decrease of R_c the square-gradient terms in the expression for the mean free path compete with the standard terms proportional to $\sigma \xi(x)$ and $\sigma \xi'(x)$.

One should stress that our approach is restricted by a first-order approximation, with a careful analysis of all terms that may be important in this approximation and taking into account an unexpectedly strong influence of the square-gradient terms. Our goal is to study this scattering mechanism and establish the conditions when it should not be neglected. For this, we derive a correct expression for the attenuation length L_n that incorporates the contribution of the above mechanism. One should emphasize that the approach we use does not assume any special restrictions to the model parameters (such as the smoothness of surface profiles) except for general conditions of *weak scattering*.

The paper is organized as follows. In Sec. II we formulate the problem and discuss the coordinate transformation used to represent the surface scattering as the bulk one. Our approach involves an average Green's function whose longitudinal wave number is a modification of the unperturbed one. Also, all expressions corresponding to the unperturbed problem are given and discussed in this section. In Sec. III we derive a Dyson-type integral equation for the exact Green's function. From the exact expression for the scattering potential we design two Hermitian random operators. The first one is associated with both the *amplitude scattering* (AS) and *gradient scattering* (GS) mechanism, while the second one is associated only with the *square-gradient scattering* (SGS) mechanism. The former operator gives rise to the *roughness-height power* (RHP) spectrum $W(k_x)$, while the latter to the *roughness-square-gradient power* (RSGP) spectrum $T(k_x)$.

In Sec. IV we obtain the averaged Green's function by applying a perturbative method with respect to the above operators. Since in this work we restrict ourselves to an

analysis of the attenuation length L_n of the n th conducting mode, we focus our attention on the imaginary part of the proper self-energy. In Sec. V, in correspondence with a clear independence between the AS+GS and SGS mechanisms, we develop a natural approach to define two attenuation lengths, the well-known one $L_n^{(1)}$ and our SGS length $L_n^{(2)}$. These two lengths are related to the RHP and RSGP spectrum, and as a consequence, they are characterized by σ^2 and σ^4 dependences, respectively. We study their interplay for two limit cases of the roughness surface, for small-scale and large-scale roughness. We discuss here the main result according to which the larger roughness slope σ/R_c , the larger contribution of the SGS mechanism. We also present a numerical analysis assuming that the surface profile $\xi(x)$ has the standard Gaussian binary correlator. Finally, in Sec. VI we outline our conclusions. A short presentation of main results can be found in Ref. 20.

II. PROBLEM FORMULATION

In what follows, we consider a standard model of an open quasi-one-dimensional waveguide (or conducting wire) of average width d , stretched along the x axis. For simplicity, one (lower) boundary of the waveguide is assumed to be flat, $z=0$, while the other (upper) boundary has a rough profile, $z=d+\sigma \xi(x)$, with σ as the root-mean-square roughness height. In other words, the waveguide occupies the region

$$-\infty \leq x \leq \infty, \quad 0 \leq z \leq w(x) \quad (2.1)$$

of the (x, z) plane. Here the fluctuating wire width $w(x)$ is defined by

$$w(x) = d + \sigma \xi(x), \quad \langle w(x) \rangle = d. \quad (2.2)$$

The random function $\xi(x)$ describes the roughness of the upper boundary. It is assumed to be a statistically homogeneous and isotropic *Gaussian* random process with the zero mean and unit variance,

$$\langle \xi(x) \rangle = 0, \quad \langle \xi^2(x) \rangle = 1, \quad \langle \xi(x) \xi(x') \rangle = \mathcal{W}(x - x'). \quad (2.3)$$

Here the angular brackets stand for statistical averaging over different realizations of the surface profile $\xi(x)$. We also assume that its binary correlator $\mathcal{W}(x)$ decreases on the scale R_c and is normalized to 1, $\mathcal{W}(0)=1$.

The roughness-height power spectrum $W(k_x)$ is defined by

$$W(k_x) = \int_{-\infty}^{\infty} dx \exp(-ik_x x) \mathcal{W}(x). \quad (2.4)$$

Since $\mathcal{W}(x)$ is an even function of x , its Fourier transform (2.4) is an even, real, and non-negative function of k_x . The RHP spectrum has a maximum at $k_x=0$ with $W(0) \sim R_c$ and decreases on the scale R_c^{-1} .

In order to analyze the surface scattering problem we shall employ the method of the retarded Green's function $\mathcal{G}(x, x'; z, z')$. Specifically, we start with the Dirichlet boundary-value problem

$$\left(\frac{\partial^2}{\partial x^2} + \frac{\partial^2}{\partial z^2} + k^2\right)\mathcal{G}(x, x'; z, z') = \delta(x - x')\delta(z - z'), \quad (2.5a)$$

$$\mathcal{G}(x, x'; z = 0, z') = 0, \quad \mathcal{G}(x, x'; z = d + \sigma\xi(x), z') = 0. \quad (2.5b)$$

Here $\delta(x)$ and $\delta(z)$ are the Dirac delta functions. The wave number k is equal to ω/c for an electromagnetic wave of the frequency ω and TE polarization, propagating through a waveguide with perfectly conducting walls. For an electron quantum wire, k is the Fermi wave number within the isotropic Fermi-liquid model.

A. Coordinate transformation

Equation (2.5a) does not contain any scattering potential. In contrast with the bulk scattering, the electromagnetic and electron waves experience a perturbation due to scattering from the upper wall; therefore, the perturbation is hidden in the boundary condition (2.5b). In order to formally describe the surface scattering as a bulk one, we perform the canonical transformation to new coordinates,

$$x_{new} = x_{old}, \quad (2.6a)$$

$$z_{new} = \frac{d}{w(x)}z_{old} = \frac{d}{d + \sigma\xi(x)}z_{old}, \quad (2.6b)$$

in which both waveguide surfaces are flat. Correspondingly, we introduce the canonically conjugate Green's function (below for convenience we drop the subscript *new* for x and z),

$$\mathcal{G}_{new}(x, x'; z, z') = \frac{\sqrt{w(x)w(x')}}{d}\mathcal{G}_{old}(x, x'; z, z'). \quad (2.7)$$

Here the prefactor before \mathcal{G}_{old} is due to the Jacobian of the transformation to new variables. As a result, we arrive at the equivalent boundary-value problem governed by the equation

$$\left(\frac{\partial^2}{\partial x^2} + \frac{\partial^2}{\partial z^2} + k^2\right)\mathcal{G}(x, x'; z, z') - \hat{U}(x, z)\mathcal{G}(x, x'; z, z') = \delta(x - x')\delta(z - z'), \quad (2.8a)$$

$$\mathcal{G}(x, x'; z = 0, z') = 0, \quad \mathcal{G}(x, x'; z = d, z') = 0. \quad (2.8b)$$

Here the effective *surface scattering potential* $\hat{U}(x, z)$ is given by the expression

$$\hat{U}(x, z) = \left[1 - \frac{d^2}{w^2(x)}\right]\frac{\partial^2}{\partial z^2} + \frac{\sigma}{w(x)}\left[\xi''(x) + 2\xi'(x)\frac{\partial}{\partial x}\right] \times \left[\frac{1}{2} + z\frac{\partial}{\partial z}\right] - \frac{\sigma^2\xi'^2(x)}{w^2(x)}\left[\frac{3}{4} + 3z\frac{\partial}{\partial z} + z^2\frac{\partial^2}{\partial z^2}\right]. \quad (2.9)$$

Note that the prime over the function $\xi(x)$ denotes a derivative with respect to x . It is important to stress that Eqs. (2.8)

and (2.9) are *exact* and valid for any form of the surface profile $\xi(x)$.

B. Unperturbed Green's function

The unperturbed Green's function $\mathcal{G}_0(|x - x'|; z, z')$ obeys the boundary-value problem (2.8) with $\hat{U}(x, z) = 0$ [when $\sigma = 0$, and therefore, $w(x) = d$]. It is determined as follows:

$$\mathcal{G}_0(|x - x'|; z, z') = \int_{-\infty}^{\infty} \frac{dk_x dk'_x}{(2\pi)^2} \exp[i(k_x x - k'_x x')] \times g_0(k_x, k'_x) \frac{\sin(k_z z)\sin(k'_z z')}{k_z k'_z} \quad (2.10a)$$

$$= \sum_{n=1}^{N_d} \sin\left(\frac{\pi n z}{d}\right) \sin\left(\frac{\pi n z'}{d}\right) \frac{\exp(ik_n |x - x'|)}{ik_n d}. \quad (2.10b)$$

Here k_x and k_z are the lengthwise and transverse wave numbers,

$$k_z = k_z(k_x) = \sqrt{k^2 - k_x^2}, \quad k'_z = k'_z(k'_x). \quad (2.11)$$

Their unperturbed eigenvalues are k_n ,

$$k_n = \sqrt{k^2 - (\pi n/d)^2}, \quad n = 1, 2, 3, \dots, N_d, \quad (2.12)$$

and $\pi n/d$, respectively. The total number N_d of propagating waveguide modes (conducting channels that have real values of k_n) is determined by the integer part $[\dots]$ of the ratio kd/π ,

$$N_d = [kd/\pi]. \quad (2.13)$$

The first expression (2.10a) gives the unperturbed Green's function in the *pole representation* where $g_0(k_x, k'_x)$ is called the *pole factor*,

$$g_0(k_x, k'_x) = 2\pi\delta(k_x - k'_x)g_0(k_x), \quad (2.14a)$$

$$g_0(k_x) = k_z \cot(k_z d) \rightarrow \quad (2.14b)$$

$$\sum_{n=1}^{N_d} \frac{(\pi n/d)^2}{k_n d} \left(\frac{1}{k_x + k_n + i0} - \frac{1}{k_x - k_n - i0} \right). \quad (2.14c)$$

The evaluation of the integrals in Eq. (2.10a) over the poles of $g_0(k_x, k'_x)$ results in the mode representation (2.10b) for the unperturbed Green's function.

Note that the sums in Eqs. (2.10b) and (2.14c) run only over the *propagating modes* with $n \leq N_d$ and ignore the contribution of *evanescent modes*, which have mode indices $n > N_d$. The reasons of such neglect are the following: (i) The evanescent modes have purely imaginary wave number k_n and therefore do not contribute to the transport of waveguiding structures. (ii) They exponentially decay over the wavelength and hence are not sensitive to any scattering potential. (iii) As one can see below, in the considered approximation the attenuation length L_n is determined by the imaginary part of the pole factor $g_0(k_x)$, which is formed solely by the propagating modes.

III. DYSON EQUATION

With the use of the Green's theorem, it can be easily shown that the boundary-value problem (2.8) is directly reduced to the following *exact* Dyson-type integral equation

$$\begin{aligned} \mathcal{G}(x, x'; z, z') &= \mathcal{G}_0(|x - x'|; z, z') + \int_{-\infty}^{\infty} dx_1 \int_0^d dz_1 \\ &\times \mathcal{G}_0(|x - x_1|; z, z_1) \hat{U}(x_1, z_1) \mathcal{G}(x_1, x'; z_1, z'). \end{aligned} \quad (3.1)$$

This equation relates the perturbed by surface disorder Green's function $\mathcal{G}(x, x'; z, z')$ to the Green's function $\mathcal{G}_0(|x - x'|; z, z')$ of the waveguide with perfectly flat boundaries.

Similarly to the pole representation (2.10a) for the unperturbed Green's function, let us seek $\mathcal{G}(x, x'; z, z')$ in the form

$$\begin{aligned} \mathcal{G}(x, x'; z, z') &= \int_{-\infty}^{\infty} \frac{dk_x dk'_x}{(2\pi)^2} \exp[i(k_x x - k'_x x')] \\ &\times g(k_x, k'_x) \frac{\sin(k_z z) \sin(k'_z z')}{k_z k'_z}. \end{aligned} \quad (3.2)$$

With this method the problem of deriving the Green's function $\mathcal{G}(x, x'; z, z')$ is reduced to obtaining its pole factor $g(k_x, k'_x)$. To this end, we substitute the pole representations (2.10a) and (3.2) into Eq. (3.1) and get the non-local Dyson equation in the k_x representation,

$$g(k_x, k'_x) = g_0(k_x, k'_x) + \int_{-\infty}^{\infty} \frac{dq_x dq'_x}{(2\pi)^2} g_0(k_x, q_x) \Xi(q_x, q'_x) g(q'_x, k'_x). \quad (3.3)$$

In this representation the effective surface scattering potential $\Xi(k_x, k'_x)$ is

$$\begin{aligned} \Xi(k_x, k'_x) &= \int_{-\infty}^{\infty} dx_1 \int_0^d dz_1 \exp(-ik_x x_1) \frac{\sin(k_z z_1)}{k_z} \\ &\times \hat{U}(x_1, z_1) \exp(ik'_x x_1) \frac{\sin(k'_z z_1)}{k'_z}. \end{aligned} \quad (3.4)$$

Thus, we obtained the Dyson-type integral equation (3.3) with an *exact* expression (3.4) for the kernel $\Xi(k_x, k'_x)$. After the substitution of the expression (2.9) for \hat{U} , we realize that the kernel consists of three groups of terms. The first one has the factor $[1 - d^2/w^2(x_1)]$ while the second and third groups have, respectively, the factors $\sigma/w(x_1)$ and $\sigma^2/w^2(x_1)$. One needs to note that while the kernel $\Xi(k_x, k'_x)$ is Hermitian in the whole, its latter two parts are non-Hermitian individually. To have each part of $\Xi(k_x, k'_x)$ Hermitian, we perform the integration by parts for the term containing $\xi''(x_1)$ in the second group. After that we come to the final *exact* form for the perturbation potential,

$$\begin{aligned} \Xi(k_x, k'_x) &= \int_{-\infty}^{\infty} dx_1 \int_0^d dz_1 \exp(-ik_x x_1) \frac{\sin(k_z z_1)}{k_z} \\ &\times \left\{ \left[1 - \frac{d^2}{w^2(x_1)} \right] \frac{\partial^2}{\partial z_1^2} + i(k_x + k'_x) \frac{\sigma \xi'(x_1)}{w(x_1)} \right. \\ &\times \left[\frac{1}{2} + z_1 \frac{\partial}{\partial z_1} \right] - \frac{\sigma^2 \xi'^2(x_1)}{w^2(x_1)} \\ &\times \left. \left[\frac{1}{4} + 2z_1 \frac{\partial}{\partial z_1} + z_1^2 \frac{\partial^2}{\partial z_1^2} \right] \right\} \exp(ik'_x x_1) \frac{\sin(k'_z z_1)}{k'_z}. \end{aligned} \quad (3.5)$$

This equation has a peculiar structure very useful in further analysis. The kernel written in this form also consists of three groups of terms; however, now they represent different scattering mechanisms.

Since we are interested in the averaged Green's function, we have to calculate the binary correlator of $\Xi(k_x, k'_x)$. Therefore, to avoid very cumbersome calculations, it is reasonable to make a simplification of $\Xi(k_x, k'_x)$ that does not destroy the Hermitian structure of each group of terms. To this end and taking into account that our interest is in the typical case of small surface corrugations ($\sigma \ll d$), we can do the following: expand the factor $1 - d^2/w^2(x_1) \approx 2\sigma\xi(x_1)/d$ in the first term of Eq. (3.5) and put $w(x_1) \approx d$ in all the others. In such a way, we get a suitable *approximate* expression for the surface scattering potential,

$$\begin{aligned} \Xi(k_x, k'_x) &\approx \int_{-\infty}^{\infty} dx_1 \int_0^d dz_1 \exp(-ik_x x_1) \frac{\sin(k_z z_1)}{k_z} \\ &\times \left\{ \frac{2\sigma\xi(x_1)}{d} \frac{\partial^2}{\partial z_1^2} + i(k_x + k'_x) \frac{\sigma\xi'(x_1)}{d} \left[\frac{1}{2} + z_1 \frac{\partial}{\partial z_1} \right] \right. \\ &- \frac{\sigma^2 \xi'^2(x_1)}{d^2} \left[\frac{1}{4} + 2z_1 \frac{\partial}{\partial z_1} + z_1^2 \frac{\partial^2}{\partial z_1^2} \right] \left. \right\} \\ &\times \exp(ik'_x x_1) \frac{\sin(k'_z z_1)}{k'_z}. \end{aligned} \quad (3.6)$$

Expression (3.6) contains one term that depends on the *amplitude* of the roughness profile $\sigma\xi(x_1)$ and two groups of terms that depend on the roughness *gradient* $\sigma\xi'(x_1)$ and the roughness *square-gradient* $\sigma^2\xi'^2(x_1)$ terms, respectively. An interesting point to mention is that the last group, due to its proportionality to σ^2 , was neglected in all previous studies of the transport properties of surface-disordered waveguides. However, as we show below, the scattering due to these terms has properties very different from those described by other terms and should be properly taken into account.

In order to proceed further, we assert that the kernel can be written as the sum of its average, $\langle \Xi(k_x, k'_x) \rangle$, and fluctuating, $\tilde{\Xi}(k_x, k'_x)$, parts—i.e.,

$$\Xi(k_x, k'_x) = \langle \Xi(k_x, k'_x) \rangle + \tilde{\Xi}(k_x, k'_x). \quad (3.7)$$

It can be tested that the average $\langle \Xi(k_x, k'_x) \rangle$ contributes only to the real part γ_n of the complex renormalization δk_n of the lengthwise wave number k_n [see Eq. (1.1)] and therefore,

does not change static transport properties of the surface disordered waveguide. Thus, we will omit it because our interest is in the attenuation length L_n , not in γ_n .

From Eq. (3.6) one can see that all terms with the linear dependence on σ have zero mean value. Therefore, the average part $\langle \Xi(k_x, k'_x) \rangle$ of the kernel $\Xi(k_x, k'_x)$ is associated only with the group of terms containing $\sigma^2 \xi'^2(x_1)$. To extract their fluctuating contribution, we should subtract from $\xi'^2(x_1)$ its mean value $\langle \xi'^2(x_1) \rangle$. In such a way, we introduce the following zero-mean-valued *square-gradient function*

$$\mathcal{V}(x) = \xi'^2(x) - \langle \xi'^2(x) \rangle, \quad \langle \mathcal{V}(x) \rangle = 0. \quad (3.8)$$

The function $\mathcal{V}(x)$ plays a special role in our further consideration. In accordance with the Gaussian nature of the surface-profile function $\xi(x)$, the function $\hat{\mathcal{V}}(x)$ is uncorrelated with both $\xi(x)$ and $\xi'(x)$,

$$\langle \xi(x) \mathcal{V}(x') \rangle = 0, \quad \langle \xi'(x) \mathcal{V}(x') \rangle = 0. \quad (3.9)$$

Its pair correlator is given by

$$\langle \mathcal{V}(x) \mathcal{V}(x') \rangle = 2 \langle \xi'(x) \xi'(x') \rangle^2 = 2 \mathcal{W}''^2(x - x'). \quad (3.10)$$

Since we use the k_x representation, it is worthwhile to define the Fourier transform of $\mathcal{V}(x)$,

$$V(k_x) = \int_{-\infty}^{\infty} dx \exp(-ik_x x) \mathcal{V}(x). \quad (3.11)$$

Also, we need the correlator of its Fourier transform,

$$\langle V(k_x) V(k'_x) \rangle = 4\pi \delta(k_x + k'_x) T(k_x). \quad (3.12)$$

Here the roughness-square-gradient power spectrum $T(k_x)$ is

$$T(k_x) = \int_{-\infty}^{\infty} dx \exp(-ik_x x) \mathcal{W}''^2(x). \quad (3.13)$$

One should stress that, on the one hand, through the integration by parts, the power spectrum of the roughness gradients $\xi'(x)$ can be reduced to the RHP spectrum $W(k_x)$. On the other hand, it is not possible to do the same for the RSGP spectrum $T(k_x)$. This very fact reflects a highly nontrivial role of the SGS, giving rise to its competition with the well-known scattering mechanism, in spite of the seeming smallness of the term $\sigma^2 \xi'^2(x)$.

With the introduction of $V(k_x)$ we are ready to explicitly write down the fluctuating part of the total scattering potential,

$$\tilde{\Xi}(k_x, k'_x) = \Xi_1(k_x, k'_x) + \Xi_2(k_x, k'_x). \quad (3.14)$$

The first summand is associated with the first and second terms in Eq. (3.6),

$$\begin{aligned} \Xi_1(k_x, k'_x) &= \int_{-\infty}^{\infty} dx_1 \int_0^d dz_1 \exp(-ik_x x_1) \frac{\sin(k_z z_1)}{k_z} \\ &\times \left\{ \frac{2\sigma \xi(x_1)}{d} \frac{\partial^2}{\partial z_1^2} + i(k_x + k'_x) \frac{\sigma \xi'(x_1)}{d} \right. \\ &\times \left. \left[\frac{1}{2} + z_1 \frac{\partial}{\partial z_1} \right] \right\} \exp(ik'_x x_1) \frac{\sin(k'_z z_1)}{k'_z} \end{aligned} \quad (3.15a)$$

$$= -\sigma [A(k_x, k'_x) + B(k_x, k'_x)] \tilde{\xi}(k_x - k'_x). \quad (3.15b)$$

The second summand is related to the third term in Eq. (3.6), with $\xi'^2(x_1)$ being replaced by $\mathcal{V}(x_1)$,

$$\begin{aligned} \Xi_2(k_x, k'_x) &= - \int_{-\infty}^{\infty} dx_1 \int_0^d dz_1 \exp(-ik_x x_1) \frac{\sin(k_z z_1)}{k_z} \\ &\times \frac{\sigma^2 \mathcal{V}(x_1)}{d^2} \left[\frac{1}{4} + 2z_1 \frac{\partial}{\partial z_1} + z_1^2 \frac{\partial^2}{\partial z_1^2} \right] \\ &\times \exp(ik'_x x_1) \frac{\sin(k'_z z_1)}{k'_z} \end{aligned} \quad (3.16a)$$

$$= \sigma^2 D(k_x, k'_x) V(k_x - k'_x). \quad (3.16b)$$

In Eq. (3.15) the quantity $\tilde{\xi}(k_x)$ is the Fourier transform of the function $\xi(x)$,

$$\tilde{\xi}(k_x) = \int_{-\infty}^{\infty} dx \exp(-ik_x x) \xi(x). \quad (3.17)$$

Also, we have introduced the following quantities in the first summand:

$$A(k_x, k'_x) = \frac{2k'_z}{k_z d} \int_0^d dz \sin(k_z z) \sin(k'_z z), \quad (3.18a)$$

$$A(\pm k_n, \pm k_{n'}) = \delta_{nn'}, \quad (3.18b)$$

$$B(k_x, k'_x) = \frac{k_x^2 - k'_x{}^2}{d} \int_0^d dz \frac{\sin(k_z z)}{k_z} \left[\frac{1}{2} + z \frac{\partial}{\partial z} \right] \frac{\sin(k'_z z)}{k'_z}, \quad (3.19a)$$

$$B(\pm k_n, \pm k_{n'}) = \cos[\pi(n - n')] (1 - \delta_{nn'}). \quad (3.19b)$$

In the last expression we have used the equality

$$k_x^2 - k'_x{}^2 = -(k_z^2 - k'_z{}^2), \quad (3.20)$$

which directly follows from the energy conservation $k^2 = k_x^2 + k_z^2 = k'_x{}^2 + k'_z{}^2$ [see the definition (2.11)]. And finally, in the second summand the following factors appeared:

$$\begin{aligned} D(k_x, k'_x) &= - \frac{1}{d^2} \int_0^d dz \frac{\sin(k_z z)}{k_z} \\ &\times \left[\frac{1}{4} + 2z \frac{\partial}{\partial z} + z^2 \frac{\partial^2}{\partial z^2} \right] \frac{\sin(k'_z z)}{k'_z}, \end{aligned} \quad (3.21a)$$

$$D(\pm k_n, \pm k_{n'}) = \frac{d}{2} \left[\frac{1}{3} + \frac{1}{(2\pi n)^2} \right] \delta_{nn'} + \frac{2d}{\pi^2} \frac{n^2 + n'^2}{(n^2 - n'^2)^2} \times \cos[\pi(n - n')](1 - \delta_{nn'}). \quad (3.21b)$$

The operator $\tilde{\Xi}(k_x, k'_x)$ written as the sum (3.14) of specially designed terms has a very convenient form. First, both terms are chosen to have zero average. Second, since the functions $\xi(x)$ and $\mathcal{V}(x)$ do not correlate with each other [see Eq. (3.9)], their Fourier transforms are also uncorrelated,

$$\langle \tilde{\xi}(k_x) \mathcal{V}(k'_x) \rangle = 0. \quad (3.22)$$

Due to the condition (3.22), the scattering potentials $\Xi_1(k_x, k'_x)$ and $\Xi_2(k_x, k'_x)$ are also uncorrelated. However, they have the following autocorrelators:

$$\langle \Xi_1(k_x, q_x) \Xi_1(q_x, k'_x) \rangle = 2\pi \delta(k_x - k'_x) Q_1(k_x, q_x), \quad (3.23a)$$

$$Q_1(k_x, q_x) = \sigma^2 W(k_x - q_x) [A(k_x, q_x) + B(k_x, q_x)] \times [A(q_x, k_x) + B(q_x, k_x)], \quad (3.23b)$$

$$\langle \Xi_2(k_x, q_x) \Xi_2(q_x, k'_x) \rangle = 2\pi \delta(k_x - k'_x) Q_2(k_x, q_x), \quad (3.24a)$$

$$Q_2(k_x, q_x) = 2\sigma^4 T(k_x - q_x) D(k_x, q_x) D(q_x, k_x). \quad (3.24b)$$

As a result, the correlator of the fluctuating scattering potential (3.14) in the k_x representation is as follows:

$$\langle \tilde{\Xi}(k_x, q_x) \tilde{\Xi}(q_x, k'_x) \rangle = 2\pi \delta(k_x - k'_x) Q(k_x, q_x), \quad (3.25a)$$

$$Q(k_x, q_x) = Q_1(k_x, q_x) + Q_2(k_x, q_x). \quad (3.25b)$$

It is now possible to perform an appropriate perturbative averaging of the Dyson equation (3.3) and, at the same time, to separate a relative contribution of the SGS mechanism from the total scattering process.

IV. AVERAGE GREEN'S FUNCTION

Now we are in a position to replace the problem for the random Green's function $\mathcal{G}(x, x'; z, z')$ with the problem for the Green's function $\langle \mathcal{G}(x, x'; z, z') \rangle$ averaged over the surface disorder. It is evident that $\langle \mathcal{G}(x, x'; z, z') \rangle$ is governed by Eq. (3.2) with the average pole factor $\langle g(k_x, k'_x) \rangle$ instead of the random one. To perform the averaging of Eq. (3.3) with $\Xi(k_x, k'_x)$ given by Eq. (3.14) and obtain $\langle g(k_x, k'_x) \rangle$, we can apply one of the standard and well-known perturbative methods. For example, it can be the diagrammatic approach developed for surface disordered systems,¹ as well as the technique developed in Ref. 3. Both of the methods allow one to develop a consistent perturbative approach with respect to the scattering potential that takes adequately into account the *multiple scattering* from the corrugated boundary. Then, we come to the following result:

$$\langle g(k_x, k'_x) \rangle = g_0(k_x, k'_x) + \int_{-\infty}^{\infty} \frac{dq_x dq'_x dq''_x dq'''_x}{(2\pi)^4} g_0(k_x, q_x) \times \langle \tilde{\Xi}(q_x, q'_x) g_0(q'_x, q''_x) \tilde{\Xi}(q''_x, q'''_x) \rangle \langle g(q'''_x, k'_x) \rangle. \quad (4.1)$$

Taking into account the presence of δ functions in the definitions (2.14a) for the unperturbed pole factor and in Eq. (3.25a) for the scattering potential, we can take explicitly the integrals over q_x , q''_x , and q'''_x in the second term. After that, Eq. (4.1) becomes an algebraic one. Its solution has the form

$$\langle g(k_x, k'_x) \rangle = 2\pi \delta(k_x - k'_x) g(k_x), \quad (4.2a)$$

$$g(k_x) = [g_0^{-1}(k_x) - M(k_x)]^{-1}. \quad (4.2b)$$

The quantity $M(k_x)$ is called the *self-energy or mass operator*. It is described by the formula

$$M(k_x) = \int_{-\infty}^{\infty} \frac{dq_x}{2\pi} Q(k_x, q_x) g_0(q_x). \quad (4.3)$$

One should recall that when obtaining Eq. (4.1) we have omitted the average part of the kernel, $\Xi(k_x, k'_x)$. The motivation to discard it, as was stated after Eq. (3.7), arises because its contribution to the renormalization of the lengthwise wave number k_n is real; i.e., it contributes only to the quantity γ_n [see Eq. (1.1)]. Besides this, another contribution to γ_n arises due to the real part of the self-energy. For this reason, we can expand the average pole factor $g(k_x)$ in series of partial fractions and retain only the imaginary part of the self-energy $M(k_n)$,

$$g(k_x) \rightarrow \sum_{n=1}^{N_d} \frac{(\pi n/d)^2}{k_n d} \left(\frac{1}{k_x + k_n + i/2L_n} - \frac{1}{k_x - k_n - i/2L_n} \right). \quad (4.4)$$

This expression completely corresponds to the representation (2.14c) for the unperturbed pole factor. It is suitable for further evaluation of the average Green's function.

The quantity L_n is the *total wave attenuation length* or electron *mean free path* of the n th conducting mode. It describes the scattering from the n th mode into all possible propagating modes. This quantity is determined by the imaginary part of the self-energy $M(k_n)$,

$$L_n^{-1} = -2 \frac{(\pi n/d)^2}{k_n d} \text{Im} M(k_n) \quad (4.5a)$$

$$= \frac{(\pi n/d)^2}{k_n d} \sum_{n'=1}^{N_d} \frac{(\pi n'/d)^2}{k_{n'} d} \times [Q(k_n, -k_{n'}) + Q(k_n, +k_{n'})]. \quad (4.5b)$$

Let us substitute Eqs. (4.2a) and (4.4) into Eq. (3.2) and perform straightforward calculations of the integrals with the use of the δ function and over the poles of $g(k_x)$. As a result, we find the average Green's function

$$\langle \mathcal{G}(x, x'; z, z') \rangle = \bar{\mathcal{G}}(|x - x'|; z, z'), \quad (4.6)$$

in the efficient representation via canonical Fourier series in the normal waveguide modes,

$$\begin{aligned} \bar{\mathcal{G}}(|x - x'|; z, z') &= \sum_{n=1}^{N_d} \sin\left(\frac{\pi n z}{d}\right) \sin\left(\frac{\pi n z'}{d}\right) \\ &\times \frac{\exp(ik_n |x - x'|)}{ik_n d} \exp\left(-\frac{|x - x'|}{2L_n}\right). \end{aligned} \quad (4.7)$$

V. ATTENUATION LENGTH ANALYSIS

In view of Eq. (3.25b), the general expression (4.5) for the inverse attenuation length shows that in the problem under consideration this quantity consists of two terms,

$$\frac{1}{L_n} = \frac{1}{L_n^{(1)}} + \frac{1}{L_n^{(2)}}. \quad (5.1)$$

These terms descend from different mechanisms of the surface scattering. The first attenuation length $L_n^{(1)}$ is related to the RHP spectrum $W(k_x)$ through the expression for $Q_1(k_x, k'_x)$. In accordance with Eqs. (3.23b), (3.18b), and (3.19b), it is given by

$$\frac{1}{L_n^{(1)}} = \sigma^2 \frac{(\pi n/d)^2}{k_n d} \sum_{n'=1}^{N_d} \frac{(\pi n'/d)^2}{k_{n'} d} [W(k_n + k_{n'}) + W(k_n - k_{n'})]. \quad (5.2)$$

Its *diagonal term* is formed by the *amplitude scattering*, and the *off-diagonal terms* result from the *gradient scattering*. These two mechanisms of surface scattering are due to the corresponding terms in the expression for $\Xi_1(k_x, k'_x)$ [see Eq. (3.15a)]—i.e., the former from the term depending on the *amplitude* of the roughness profile $\sigma\xi(x)$ and the latter from the terms depending on the roughness *gradient* $\sigma\xi'(x)$. Expression (5.2) exactly coincides with that previously obtained by various methods (see, e.g., Ref. 1).

The second attenuation length $L_n^{(2)}$ related to the RSGP spectrum through $Q_2(k_x, k'_x)$ is associated solely with the SGS mechanism due to the square-gradient function $\mathcal{V}(x)$ [see Eq. (3.16a)]. In accordance with Eqs. (3.24b) and (3.21b), it is described by

$$\frac{1}{L_n^{(2)}} = \sum_{n'=1}^{N_d} \frac{1}{L_{nn'}^{(2)}}. \quad (5.3)$$

Here its diagonal term controlling the wave scattering inside the mode (*intramode scattering*) is written as

$$\frac{1}{L_{nn}^{(2)}} = \frac{\sigma^4 (\pi n/d)^4}{2 k_n^2} \left[\frac{1}{3} + \frac{1}{(2\pi n)^2} \right]^2 [T(2k_n) + T(0)]. \quad (5.4)$$

The off-diagonal partial scattering length $L_{n \neq n'}^{(2)}$ that de-

scribes the *intermode scattering* [from the n th mode to the (n')th one, $n \neq n'$] is

$$\begin{aligned} \frac{1}{L_{n \neq n'}^{(2)}} &= \frac{8\sigma^4 (\pi n/d)^2 (\pi n'/d)^2 (n^2 + n'^2)^2}{\pi^4 k_n k_{n'} (n^2 - n'^2)^4} \\ &\times [T(k_n + k_{n'}) + T(k_n - k_{n'})]. \end{aligned} \quad (5.5)$$

To the best of our knowledge, in the surface-scattering problem for multimode waveguides the square-gradient function $\mathcal{V}(x)$ was never taken into account, and as a result, the second attenuation length, or SGS length, $L_n^{(2)}$, was missed in previous studies.

Now we list the simplifications that have been made in deriving Eqs. (5.1)–(5.5) for the attenuation length L_n . First, the proper self-energy (4.3) in the Dyson-type equation for the average Green's function has been obtained within the second-order approximation in the perturbation potential. In terms of the diagrammatic technique this is similar to the “simple vortex” or, the same, Bourret approximation,²¹ which contains the binary correlator $Q(k_x, q_x)$ of the surface-scattering potential and the unperturbed pole factor $g_0(q_x)$. To find out the conditions of applicability for this approach, we have used the ideas proposed in the book 2. More specifically, we substitute into the self-energy (4.3) the average pole factor (4.2b) instead of the unperturbed one. This trick is equivalent to the summation of an infinite subsequence of diagrams in the exact expansion of the self-energy in powers of the scattering potential. The analysis shows that in the Dyson-type equation the new (and more general) self-energy can be reduced to ours, if the channel broadening $1/2L_n$ is much less than the unperturbed quantum wave number k_n and the variation scale R_c^{-1} of the RHP and RSGP spectra—i.e., when $2k_n L_n \gg 1$ and $R_c \ll 2L_n$.

Second, in order to extract the inverse attenuation length from the self-energy (4.3), we have changed the lengthwise wave number k_x by its unperturbed value k_n . This change is justified if the surface-induced broadening $1/2L_n$ can be neglected in comparison with R_c^{-1} and the spacing $|k_n - k_{n \pm 1}| \approx |\partial k_n / \partial n|$ between neighboring quantum wave numbers. Now we take into account that $|\partial k_n / \partial n| \sim \Lambda_n^{-1}$, where Λ_n is the distance between two successive reflections of the n th mode from the rough boundary. Therefore, the use of k_n instead of k_x in the argument of the self-energy is valid under the conditions $R_c \ll 2L_n$ and $\Lambda_n \ll 2L_n$.

Thus, we come to three requirements: $R_c \ll 2L_n$, $\Lambda_n \ll 2L_n$, and $2k_n L_n \gg 1$. Due to the obvious relationship $k_n \Lambda_n \geq 1$, the last inequality is a direct consequence of the second one and one can conclude that the domain of applicability for our results is restricted by two independent criteria of *weak surface scattering*,

$$\Lambda_n = 2k_n d / (\pi n/d) \ll 2L_n, \quad R_c \ll 2L_n. \quad (5.6)$$

They imply that the wave is weakly attenuated on both the correlation length R_c and the cycle length Λ_n . From the analysis performed above, it becomes clear that expressions (5.2)–(5.5) represent main contributions from the substantially distinct surface-scattering mechanisms: AS+GS and SGS. In particular, the corrections that are proportional to σ^4 ,

TABLE I. Evaluation of Eq. (5.11).

n	Δn							
	-4	-3	-2	-1	1	2	3	4
1	0.002	0.006	0.024	0.31				
2	...	0.004	0.019	0.27	0.31			
3	0.018	0.26	0.27	0.024		
4	0.26	0.26	0.019	0.006	
5	0.26	0.018	0.004	0.002
⋮								

originating from the next order of approximation in the *amplitude* and *gradient* terms of the surface-scattering potential, cannot compete with the main contribution (5.2) under the conditions (5.6). On the contrary, the *square-gradient* terms give rise to the σ^4 terms in Eqs. (5.4) and (5.5), which should not be neglected due to a specific dependence on the correlation length R_c . Note that Eq. (5.6) implicitly includes the requirement that $\sigma \ll d$ for the surface corrugations be small in height, which has been employed in Sec. III when deriving the explicit form (3.6) for the surface scattering potential $\Xi(k_x, k'_x)$.

We are now in a position to analyze the attenuation length L_n . For convenience, in our further analysis, we deal with attenuation lengths in the form of the dimensionless quantities $\Lambda_n/2L_n$, $\Lambda_n/2L_n^{(1)}$, and $\Lambda_n/2L_n^{(2)}$. Since $L_n^{(1)}$ and $L_n^{(2)}$ depend on as many as four dimensionless parameters $(k\sigma)^2$, kR_c , kd/π , and n , the complete analysis appears to be quite complicated. For this reason, below we restrict ourselves to an analysis of the interplay between $L_n^{(1)}$ and $L_n^{(2)}$ as a function of the dimensionless correlation length kR_c , for different values of $(k\sigma)^2$ and mode index n . In the analysis, we consider a multimode waveguide—i.e., the situation when the number of propagating modes is large, $N_d \approx kd/\pi \gg 1$. From the physical point of view, two types of rough surfaces seem to be the most important. Surfaces of the first type contain a small-scale roughness of the “white noise” kind when $kR_c \ll 1$. For the second type, the waveguide surface consists of large-scale random corrugations when $kR_c \gg 1$. We shall develop our analysis for these two types of surfaces.

A. Small-scale roughness

Let us start with a relatively simple and widely used case of a *small-scale boundary perturbation*, when $kR_c \ll 1$ and the surface roughness can be regarded as a δ -correlated random process with the correlator $\mathcal{W}(x-x') \approx W(0)\delta(x-x')$ and constant power spectrum $W(k_x) \approx W(0) \sim R_c$. Taking into account the evident relationship $k\Lambda_n \approx 1$, one can get the following inequalities to specify this case:

$$kR_c \ll 1 \approx k\Lambda_n. \quad (5.7)$$

It is necessary to underline that in the regime of small-scale roughness (5.7) the second of the weak-scattering conditions in Eq. (5.6) is not so restrictive as the first one and directly stems from it, $R_c \ll \Lambda_n \ll 2L_n$.

In Eqs. (5.2), (5.4), and (5.5) for the attenuation lengths the argument of the correlators $W(k_x)$ and $T(k_x)$ turns out to be much less than the scale of their decrease R_c^{-1} under the conditions (5.7). Therefore, for any term in the summation over n' the argument can be taken as zero.

Therefore, the first attenuation length is determined as follows:

$$\frac{\Lambda_n}{2L_n^{(1)}} \approx 2(k\sigma)^2 \frac{n}{kd/\pi} \frac{W(0)}{k} \sum_{n'=1}^{N_d} \frac{(\pi n'/d)^2}{k_n d} \quad (5.8a)$$

$$\approx (k\sigma)^2 \frac{n}{kd/\pi} \frac{kW(0)}{2}. \quad (5.8b)$$

Due to a large number of the conducting modes, $N_d \approx kd/\pi \gg 1$, we can change the summation over n' by integration. In this way one can obtain Eq. (5.8b) from Eq. (5.8a). In order to correctly estimate the result, one can take into account the formula

$$W(0) = \int_{-\infty}^{\infty} dx \mathcal{W}(x) = 2R_c \int_0^{\infty} d\rho \mathcal{W}(R_c \rho), \quad (5.9)$$

which directly follows from the definition (2.4) for the Fourier transform $W(k_x)$ of the binary correlator $\mathcal{W}(x)$. The function $\mathcal{W}(R_c \rho)$ is the dimensionless correlator of the dimensionless variable ρ , with the scale of decrease of the order of 1. As a result, the function $\mathcal{W}(R_c \rho)$ does not depend on R_c . Therefore, the integral over ρ entering Eq. (5.9) is a positive constant of the order of unity. For example, $W(0) = \sqrt{2\pi}R_c$ and the integral is $\sqrt{\pi}/2$ in the case of Gaussian correlations [see Eq. (5.27)].

For the SGS length we have

$$\begin{aligned} \frac{\Lambda_n}{2L_n^{(2)}} &\approx \pi^2 \frac{(k\sigma)^4}{k_n d} \frac{n^3}{(kd/\pi)} \frac{T(0)}{k^3} \\ &\times \left\{ \left[\frac{1}{3} + \frac{1}{(2\pi n)^2} \right]^2 + \frac{16k_n d}{\pi^4 (\pi n/d)^2} \right. \\ &\times \left. \left(\sum_{n'=1}^{n-1} + \sum_{n'=n+1}^{N_d} \right) \frac{(\pi n'/d)^2 (n^2 + n'^2)^2}{k_n d (n^2 - n'^2)^4} \right\} \end{aligned} \quad (5.10a)$$

$$\approx \frac{\pi^2 (k\sigma)^4}{4} \frac{n^3}{k_n d} \frac{T(0)}{(kd/\pi) k^3}. \quad (5.10b)$$

In Eq. (5.10a) every term in the sum rapidly decreases with an increase of the absolute value of $\Delta n = n - n'$. This can be seen by making use of the following estimate:

$$\frac{(n^2 + n'^2)^2}{(n^2 - n'^2)^4} \approx \frac{1}{4(\Delta n)^4} \quad \text{for } n \gg |\Delta n|. \quad (5.11)$$

The fast decrease of the factor is supported by direct calculations; see Table I. Therefore, the sum in Eq. (5.10a) can be well evaluated by two terms with $n' = n \pm 1$. For simplicity, in Eq. (5.10b) we assume $N_d \gg n \gg 1$ and replace the curly braces by factor 1/4.

The explicit form for $T(0)$ directly follows from the definition (3.13) for the correlator $T(k_x)$,

$$T(0) = \int_{-\infty}^{\infty} dx \mathcal{W}^{\prime 2}(x) = R_c^{-3} \int_{-\infty}^{\infty} d\rho \left[\frac{d^2 \mathcal{W}(R_c \rho)}{d\rho^2} \right]^2. \quad (5.12)$$

If the roughness correlations are of the Gaussian form, then according to Eq. (5.28), we have $T(0) = 3\sqrt{\pi}/4R_c^3$ and the integral over ρ entering Eq. (5.12) is equal to $3\sqrt{\pi}/4$.

The relationship between the attenuation lengths is expressed by

$$\frac{L_n^{(1)}}{L_n^{(2)}} \sim (k\sigma)^2 \frac{n^2}{k_n d} (kR_c)^{-4}. \quad (5.13)$$

According to substantially different behavior of the quantities $\Lambda_n/2L_n^{(1)}$ and $\Lambda_n/2L_n^{(2)}$ with respect to kR_c , it becomes clear that they must intersect at the crossing point $(kR_c)_{cr}$. If the crossing point falls onto the present region of small-scale roughness ($kR_c \ll 1$), its dependence on the model parameters is obtained by equating to 1 expression (5.13),

$$(kR_c)_{cr}^2 \sim (k\sigma)n/\sqrt{k_n d}. \quad (5.14)$$

To the left from this point $(kR_c)_{cr}$ the SGS length prevails, $L_n^{(2)} \ll L_n^{(1)}$. To its right the main contribution is due to the first attenuation length, $L_n^{(1)} \ll L_n^{(2)}$. Expression (5.14) shows that the crossing point is smaller for smaller values of the dimensionless roughness height $k\sigma$, as well as for smaller mode indices n , or for larger values of the mode parameter kd/π .

B. Large-scale roughness: Weak correlations

The intermediate situation arises when the correlation length R_c becomes much larger than the wave length $2\pi/k$, but still remains much less than the cycle length Λ_n ,

$$1 \ll kR_c \ll k\Lambda_n. \quad (5.15)$$

As before, the first of the weak-scattering conditions (5.6) is the most restrictive; i.e., we get $R_c \ll \Lambda_n \ll 2L_n$.

Since the distance Λ_n is larger than the correlation length R_c , successive reflections of the waves from the rough surface are weakly correlated. Meantime, the distance between neighboring wave numbers k_n and $k_{n\pm 1}$ is much smaller than the variation scale R_c^{-1} of the correlators $W(k_x)$ and $T(k_x)$,

$$|k_n - k_{n\pm 1}| \approx |\partial k_n / \partial n| = 2\pi\Lambda_n^{-1} \ll R_c^{-1}. \quad (5.16)$$

This implies that the correlators $W(k_x)$ and $T(k_x)$ are smooth functions of the summation index n' . Therefore, the sum in expression (5.2) for the first attenuation length $L_n^{(1)}$ can be substituted by the integral,

$$\begin{aligned} \frac{\Lambda_n}{2L_n^{(1)}} &\approx \sigma^2 \left(\frac{\pi n}{d} \right) \int_0^{N_d} dn' \frac{(\pi n' / d)^2}{k_n' d} \\ &\times [W(k_n + k_{n'}) + W(k_n - k_{n'})] \end{aligned} \quad (5.17a)$$

$$= \frac{\sigma^2}{\pi} \left(\frac{\pi n}{d} \right) \int_{-k}^k dk_x \sqrt{k^2 - k_x^2} W(k_n - k_x). \quad (5.17b)$$

Equation (5.17) shows that the first attenuation length is contributed by scattering of a given propagating n th mode into all other propagating modes. Note that to obtain this asymptotic result we have used only the condition of weak correlations, $R_c \ll \Lambda_n$. Therefore, Eq. (5.17) provides the reduction to Eq. (5.8) for small-scale corrugations, $kR_c \ll 1$. In the case of large-scale roughness, $kR_c \gg 1$, the formula (5.17) obtained for $L_n^{(1)}$ allows further simplifications as was done in Ref. 1.

In contrast to $L_n^{(1)}$, due to a rapidly decaying factor (5.11), the SGS length $L_n^{(2)}$ can be still described by keeping tree terms only, $n' = n, n \pm 1$, in the sum in Eq. (5.3). Taking into account the estimate (5.16), for the case $N_d \gg n \gg 1$ one can write

$$\begin{aligned} \frac{\Lambda_n}{2L_n^{(2)}} &\approx \frac{\pi^2 (k\sigma)^4}{2} \frac{n^3}{k_n d} \frac{T(0) + T(2k_n)}{k^3} \\ &\times \left\{ \left[\frac{1}{3} + \frac{1}{(2\pi n)^2} \right]^2 + \frac{8}{\pi^4} \right\} \end{aligned} \quad (5.18a)$$

$$\approx \frac{\pi^2 (k\sigma)^4}{8} \frac{n^3}{k_n d} \frac{T(0) + T(2k_n)}{k^3}. \quad (5.18b)$$

In the final expression (5.18b), we have replaced the curly braces from Eq. (5.18a) by the factor 1/4. Naturally, at small-scale corrugations, $kR_c \ll 1$, the obtained result (5.18) passes into Eq. (5.10). For the large-scale roughness, when $kR_c \gg 1$, one should use Eq. (5.18) because of an arbitrary value of the parameter $k_n R_c$. We do not consider here this case in detail due to its intermediate character.

C. Large-scale roughness: Strong correlations

In the other extreme case, the correlation length R_c is very large not only in comparison with the wavelength $2\pi/k$, but also in comparison with the cycle length Λ_n ,

$$1 \lesssim k\Lambda_n \ll kR_c. \quad (5.19)$$

In this case the number of wave reflections over the correlation length R_c is large. Therefore, the successive reflections are strongly correlated to each other.

Under the inequalities (5.19) the second of the weak-scattering conditions (5.6) is the most restrictive; therefore, the condition of applicability reads as

$$\Lambda_n \ll R_c \ll 2L_n. \quad (5.20)$$

The latter requirement determines the upper limit for the value of the correlation length R_c .

Due to Eq. (5.19), the distance between neighboring wave numbers k_n and $k_{n\pm 1}$ turns out to be much larger than the variation scale R_c^{-1} of the correlators $W(k_x)$ and $T(k_x)$,

$$|k_n - k_{n\pm 1}| \approx |\partial k_n / \partial n| = 2\pi\Lambda_n^{-1} \gg R_c^{-1}. \quad (5.21)$$

This indicates that the probability of the intermode ($n' \neq n$) transitions is exponentially small and the attenuation lengths are mainly formed by the incoherent intramode ($n' = n$) scattering. Formally, at strong correlations (5.19) the correlators $W(k_x)$ and $T(k_x)$ are the sharpest functions of the summation index n' . In the sums of Eqs. (5.2) and (5.3) for the attenuation lengths the main contribution is due to the diagonal terms with $n' = n$, in which $W(2k_n)$ and $T(2k_n)$ can be neglected in comparison with $W(0)$ and $T(0)$.

Thus, the first attenuation length reads

$$\frac{\Lambda_n}{2L_n^{(1)}} \approx \frac{(k\sigma)^2}{k_n d} \frac{n^3}{(kd/\pi)^3} kW(0). \quad (5.22)$$

Correspondingly, for the SGS length one gets

$$\frac{\Lambda_n}{2L_n^{(2)}} \approx \frac{\pi^2 (k\sigma)^4}{2} \frac{n^3}{k_n d} \frac{T(0)}{k^3} \left[\frac{1}{3} + \frac{1}{(2\pi n)^2} \right]^2. \quad (5.23)$$

The ratio of the first attenuation length to the second one can be presented as

$$\frac{L_n^{(1)}}{L_n^{(2)}} \sim \frac{\Lambda_n}{2L_n^{(1)}} \left(\frac{\Lambda_n}{R_c} \right)^5 (k_n \Lambda_n)^{-2} \ll 1. \quad (5.24)$$

According to the first inequality in Eq. (5.6), to the condition (5.19) of the strong-correlations, and to the evident relationship $k_n \Lambda_n \geq 1$, we can see that the amplitude scattering length always prevails over the SGS length within the interval of strong correlations. For this reason, in the condition of applicability (5.20) one should substitute L_n by $L_n^{(1)}$. This allows one to arrive at the inequalities in the explicit form

$$k\Lambda_n \ll kR_c \ll (k\Lambda_n)(k\sigma)^{-1}(kd/\pi n). \quad (5.25)$$

D. Numerical analysis

In this subsection we perform a numerical analysis of the scattering lengths for the case when the random surface profile $\xi(x)$ has the Gaussian binary correlator,

$$\mathcal{W}(x) = \exp(-x^2/2R_c^2). \quad (5.26)$$

Then the RHP spectrum (2.4) is given by

$$W(k_x) = \sqrt{2\pi}R_c \exp(-k_x^2 R_c^2/2). \quad (5.27)$$

The RSGP spectrum $T(k_x)$, defined by Eq. (3.13), can be explicitly presented as

$$T(k_x) = \frac{\sqrt{\pi}}{16R_c^3} [(k_x R_c)^4 - 4(k_x R_c)^2 + 12] \exp[-(k_x R_c)^2/4]. \quad (5.28)$$

In Fig. 1 we display separately the behavior of $\Lambda_n/2L_n^{(1)}$ and $\Lambda_n/2L_n^{(2)}$, as a function of the dimensionless correlation parameter kR_c , comparing them with the analytically obtained asymptotics. The dashed lines are used to plot the asymptotics (5.8) and (5.10) for the region (5.7) of small-scale roughness ($kR_c \ll 1 \approx k\Lambda_n$) and expressions (5.22) and

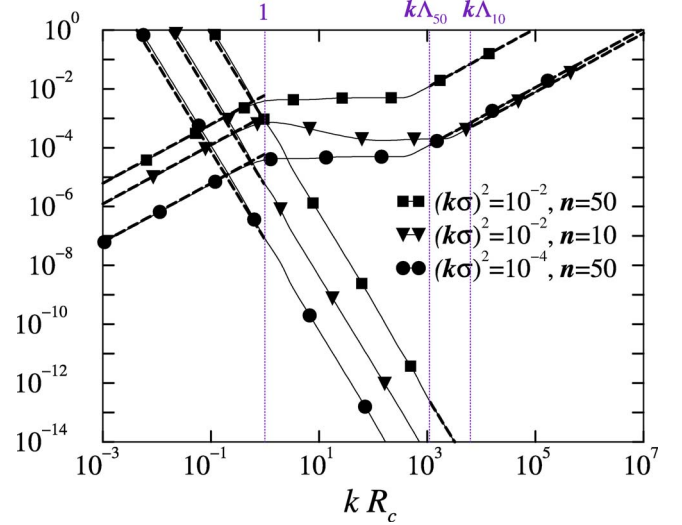


FIG. 1. (Color online) Plots of $\Lambda_n/2L_n^{(1)}$ (increasing curves) and $\Lambda_n/2L_n^{(2)}$ (decreasing curves) vs kR_c for $kd/\pi = 100.5$. Dashed lines show the corresponding asymptotic expressions.

(5.23) for the region (5.19) of large-scale roughness with strong correlations ($1 \leq k\Lambda_n \leq kR_c$). As one can see, for these two regions numerical data for both lengths are quite well described by the corresponding asymptotic expressions.

The curves $\Lambda_n/2L_n^{(1)}$ clearly manifest two transition points: between the regions of small-scale and large-scale corrugations at $kR_c \sim 1$ and between weak and strong correlations at $kR_c \sim k\Lambda_n$. As follows from Eq. (5.2), the inverse value of the first attenuation length typically increases with an increase of kR_c . Specifically, within the interval of the small-scale roughness ($kR_c \ll 1 \leq k\Lambda_n$) we have $1/L_n^{(1)} \propto kR_c$. Then, within the intermediate region of large-scale roughness with weak correlations where $1 \leq kR_c \leq k\Lambda_n$, the increase of $\Lambda_n/2L_n^{(1)}$ slows down [see the curves with the parameters $(k\sigma)^2 = 10^{-2}, 10^{-4}; n=50$] or can even be replaced by the decrease for some values of the model parameters [see the curve with the parameter $(k\sigma)^2 = 10^{-2}, n=10$]. Within these two regions, which are unified under the condition $kR_c \ll k\Lambda_n$, the quantity $1/L_n^{(1)}$ is determined by both AS and GS mechanisms (AS+GS). Finally, for large-scale roughness and strong correlations ($1 \leq k\Lambda_n \leq kR_c$) the value of $1/L_n^{(1)}$ again begins to increase linearly with kR_c . Here $1/L_n^{(1)}$ is associated solely with the AS mechanism because the main contribution to the asymptotic (5.22) is due to the diagonal term in the sum (5.2).

In contrast with $1/L_n^{(1)}$, the inverse SGS length $1/L_n^{(2)}$ reveals a monotonous decrease as the parameter kR_c increases. At small ($kR_c \leq 1 \leq k\Lambda_n$) and extremely large ($1 \leq k\Lambda_n \ll kR_c$) values of kR_c , this decrease obeys the law $1/L_n^{(2)} \propto (kR_c)^{-3}$, due to $T(0) \sim R_c^{-3}$.

In Fig. 1 we can also see the crossover from the SGS to AS+GS that is characterized by the crossing point between $\Lambda_n/2L_n^{(2)}$ and $\Lambda_n/2L_n^{(1)}$. The crossing point for two curves with the parameters $(k\sigma)^2 = 10^{-4}$ and $n=50$ is very close to that for two curves with the parameters $(k\sigma)^2 = 10^{-2}$ and $n=10$. Approximately, both crossing points are

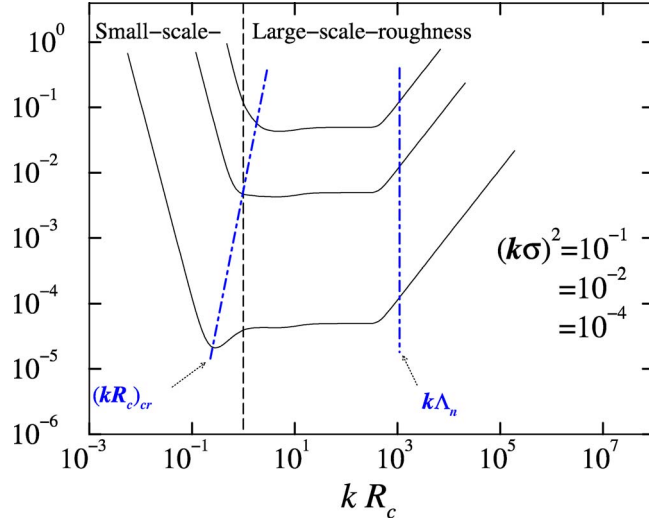


FIG. 2. (Color online) Plots of $\Lambda_n/2L_n$ versus kR_c for $kd/\pi = 100.5$, $n=50$, and different values of $(k\sigma)^2$. The dot-dashed lines labeled “ $(kR_c)_{cr}$ ” and “ $k\Lambda_n$ ” indicate the transition between the regions dominated by the SGS, AS+GS, and AS mechanisms (from the left to the right). The dashed line at $kR_c=1$ marks the transition between the regions of small-scale and large-scale roughness.

$$(kR_c)_{cr} \sim 0.2. \quad (5.29)$$

They are located well inside the interval of small-scale roughness, and their values are in agreement with the asymptotic expression (5.14). Two curves corresponding to the parameters $(k\sigma)^2=10^{-2}$ and $n=50$ have the crossing point in the transition region $kR_c \sim 1$ between small- and large-scale corrugations.

In the following two figures we display the dependence of $\Lambda_n/2L_n$ as a function of kR_c . The curves are plotted starting from the values of kR_c for which $\Lambda_n/2L_n^{(2)}=1$, according to the first condition in Eq. (5.6). Taking into account the second condition restricting the maximal value of kR_c , we plot every curve within the range where $R_c < 2L_n^{(1)}$. Based upon the description of Fig. 1, the identification of each scattering mechanism dominating in the corresponding regions becomes simple. One can see that the curves in Figs. 2 and 3 experience first a crossover from the SGS to the AS+GS and, after, from the AS+GS to AS. We outline both transitions with the labels “ $(kR_c)_{cr}$ ” and “ $k\Lambda_n$ ” respectively.

In Fig. 2 we show the dependence of $\Lambda_n/2L_n$ on kR_c for three values of the parameter $(k\sigma)^2$ [two of them $(k\sigma)^2=10^{-4}, 10^{-2}$ correspond to those used in Fig. 1]. The curve with $(k\sigma)^2=10^{-4}$ has the crossing point $(kR_c)_{cr}$ of the value (5.29) located within the interval of small-scale roughness. The crossover reveals a small dip centered at $(kR_c)_{cr}$. The curve obeys the asymptotic behavior $(kR_c)^{-3}$ to the left from $(kR_c)_{cr}$ due to the main contribution from $\Lambda_n/2L_n^{(1)}$. After, the quantity $\Lambda_n/2L_n^{(1)}$ becomes dominating in the sum (5.1); therefore, the curve begins to rise. First, the linear dependence on kR_c on the right deep side (where $kR_c < 1$) is replaced with a smoother one (for $kR_c > 1$). Finally, for $R_c > \Lambda_n$ (strong correlations) the linear dependence is restored.

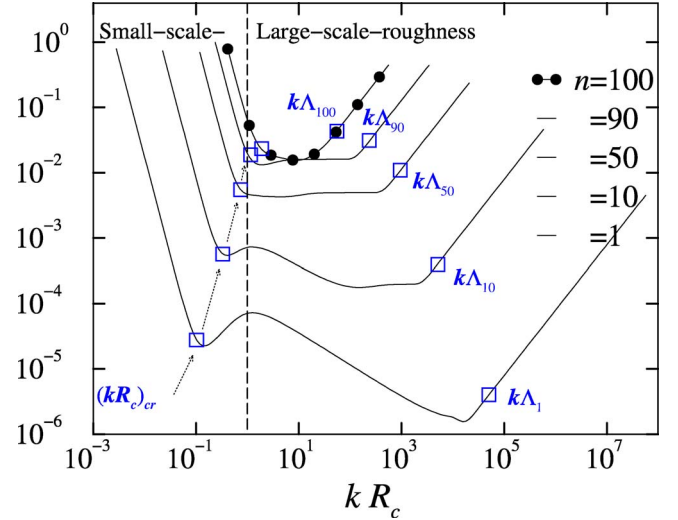


FIG. 3. (Color online) Plots of $\Lambda_n/2L_n$ versus kR_c for $kd/\pi = 100.5$, $(k\sigma)^2=10^{-2}$, and different values of the mode index n . The sets of square symbols labeled “ $(kR_c)_{cr}$ ” and “ $k\Lambda_n$ ” play the same role as dot-dashed lines in Fig. 2.

The crossing points of the second and third curves with $(k\sigma)^2=10^{-2}, 10^{-1}$ have values of the order of unity, $(kR_c)_{cr} \sim 1$. Here the total attenuation length L_n within the whole small-scale region is formed solely by the SGS length $L_n^{(2)}$. In full agreement with Eq. (5.14) the curves presented display the fact that the smaller the parameter $(k\sigma)^2$, the smaller the value of the crossing point $(kR_c)_{cr}$.

To visualize the dependence on the mode index n , in Fig. 3 we plot $\Lambda_n/2L_n$ with the parameter n spanning the range of the propagating modes. One can see that for the mode index $n=1$, the crossing point $(kR_c)_{cr} \sim 0.1$ and the curve with $n=10$ has $(kR_c)_{cr}$ given by Eq. (5.29). For the rest of the values of n the crossover occurs at $(kR_c)_{cr} \sim 1.0$. We note that the smaller the channel index n , the smaller the value of the crossing point $(kR_c)_{cr}$. This fact is in full agreement with Eq. (5.14). The squares labeled with “ $k\Lambda_n$ ” show the transition points between the AS+GS and AS mechanisms (or between the weak- and strong-correlations of the surface roughness). They are $k\Lambda_1 \approx 63\,500$, $k\Lambda_{10} \approx 6315$, $k\Lambda_{50} \approx 1100$, $k\Lambda_{90} \approx 310$, and $k\Lambda_{100} \approx 60$.

Finally, note that for all curves in our figures the roughness height is small, $\sigma/d \ll 1$. Furthermore, for the amplitude- and gradient-dominated scattering [to the right from the point $(kR_c)_{cr}$ where $\Lambda_n/2L_n^{(1)}$ mainly contributes], the average corrugation slope is also small for all data, $\sigma/R_c \ll 1$. The roughness slope remains small at the crossing points too, but increases to their left with the decrease of kR_c . As a result, to the left from the crossing point where the square-gradient term $\Lambda_n/2L_n^{(2)}$ prevails, the slope reaches the values of the order of 1, or even larger.

VI. CONCLUSION

In this paper we investigated wave and electron scattering in multimode surface-corrugated waveguides of quasi-one-

dimensional geometry. For this kind of waveguides, we have discovered a *square-gradient scattering* mechanism that is different from the previously studied ones. This mechanism arises due to specific square-gradient terms in the Hamiltonian describing the surface scattering, that are related to the *roughness square-gradient* power spectrum $T(k_x)$. Into comparison, the well-known scattering mechanisms, the *amplitude* and the *gradient* ones, are both determined by the *roughness-height* power spectrum $W(k_x)$, only. Since the SGS mechanism is independent from the others, one can define two attenuation lengths, the known length $L_n^{(1)}$ and the SGS length $L_n^{(2)}$. Both contribute to the total attenuation length (or, the same, electron mean free path) L_n according to Eq. (5.1).

The roughness-height $W(k_x)$ and square-gradient $T(k_x)$ power spectra have very different dependences on the roughness correlation length R_c . This provides a substantially different behavior of the corresponding scattering lengths in dependence of the model parameters. Specifically, the inverse value of the first attenuation length, $1/L_n^{(1)}$, typically increases, while the inverse value of the SGS length, $1/L_n^{(2)}$, decreases, with an increase of the parameter kR_c . Therefore, the curves displaying these quantities intersect upon an increase of the dimensionless correlation length kR_c , and a crossover from the SGS to AS+GS occurs. To the left from the crossing point $(kR_c)_{cr}$ the SGS length prevails over the first attenuation length, $L_n^{(2)} \ll L_n^{(1)}$. To the right from $(kR_c)_{cr}$, the first attenuation length mainly contributes to the scatter-

ing process, $L_n^{(1)} \ll L_n^{(2)}$. If the crossing point $(kR_c)_{cr}$ falls into the interval (5.7) of small-scale surface corrugations, it obeys the law (5.14).

As we have shown, at any fixed value of the root-mean-square roughness height σ , one can indicate the region of small values of the correlation length R_c where the new attenuation length $L_n^{(2)}$ predominates over the known length $L_n^{(1)}$. This predominance arises in spite of the fact that $1/L_n^{(1)}$ is proportional to σ^2 while $1/L_n^{(2)}$ is proportional to σ^4 .

In the large-scale roughness regime where the first attenuation length mainly contributes, $L_n^{(1)} \ll L_n^{(2)}$, one can observe two different behaviors of $1/L_n^{(1)}$. In the interval of weak correlations (5.15) the dependence of $1/L_n^{(1)}$ on kR_c is quite complicated, due to the coexistence of both AS and GS mechanisms. However, in the region of strong correlations (5.19), because the AS stands alone, we have much simpler behavior, $1/L_n^{(1)} \propto kR_c$. It is remarkable that the SGS mechanism prevails in the widely discussed region of a small-scale boundary perturbation, $kR_c \ll 1$, where the surface roughness is typically described via the white noise potential.

ACKNOWLEDGMENTS

This research was supported by Consejo Nacional de Ciencia y Tecnología (CONACYT, México) under Grant No. 43730 and by the Universidad Autónoma de Puebla (BUAP, México) under Grant No. 5/G/ING/05.

*Electronic address: izrailev@venus.ifuap.buap.mx

†Electronic address: makarov@siu.buap.mx

‡Electronic address: mrendon@venus.ifuap.buap.mx

¹F. G. Bass and I. M. Fuks, *Wave Scattering from Statistically Rough Surfaces* (Pergamon, New York, 1979).

²S. M. Rytov, Yu. A. Kravtsov, and V. I. Tatarskii, *Principles of Statistical Radiophysics* (Springer, Berlin, 1989).

³A. R. McGurn and A. A. Maradudin, Phys. Rev. B **30**, 3136 (1984).

⁴J. A. Sánchez-Gil, V. Freilikher, I. V. Yurkevich, and A. A. Maradudin, Phys. Rev. Lett. **80**, 948 (1998).

⁵J. A. Sánchez-Gil, V. Freilikher, A. A. Maradudin, and I. V. Yurkevich, Phys. Rev. B **59**, 5915 (1999).

⁶J. A. Konrady, J. Acoust. Soc. Am. **56**, 1687 (1974).

⁷Z. Tešanović, M. V. Jarić, and S. Maekawa, Phys. Rev. Lett. **57**, 2760 (1986).

⁸N. Trivedi and N. W. Ashcroft, Phys. Rev. B **38**, 12298 (1988).

⁹A. M. Bratkovsky and S. N. Rashkeev, Phys. Rev. B **53**, 13074 (1996).

¹⁰A. E. Meyerovich and S. Stepaniants, Phys. Rev. Lett. **73**, 316 (1994); Phys. Rev. B **51**, 17116 (1995); **58**, 13242 (1998); **60**, 9129 (1999); J. Phys.: Condens. Matter **12**, 5575 (2000).

¹¹G. A. Luna-Acosta, Kyungsun Na, L. E. Reichl, and A. Krokhin, Phys. Rev. E **53**, 3271 (1996).

¹²A. B. Isers, A. A. Puzenko, and I. M. Fuks, Akust. Zh. **36**, 454 (1990) [Sov. Phys. Acoust. **36**, 253 (1990)]; J. Electromagn. Waves Appl. **5**, 1419 (1991).

¹³N. M. Makarov and Yu. V. Tarasov, J. Phys.: Condens. Matter **10**, 1523 (1998); Phys. Rev. B **64**, 235306 (2001).

¹⁴G. A. Luna-Acosta, J. A. Méndez-Bermúdez, and F. M. Izrailev, Phys. Rev. E **64**, 036206 (2001).

¹⁵A. G. Voronovich, *Wave Scattering from Rough Surfaces* (Springer, Berlin, 1994).

¹⁶A. A. Krokhin, N. M. Makarov, and V. A. Yampol'skii, J. Phys.: Condens. Matter **3**, 4621 (1991).

¹⁷N. M. Makarov, A. V. Moroz, and V. A. Yampol'skii, Phys. Rev. B **52**, 6087 (1995).

¹⁸V. I. Tatarskii, Waves Random Media **3**, 127 (1993); **7**, 557 (1997); **10**, 339 (2000).

¹⁹A. B. Migdal, *Qualitative Methods in Quantum Theory* (Benjamin, London, 1977), p. 98.

²⁰F. M. Izrailev, N. M. Makarov, and M. Rendón, Phys. Rev. B **72**, 041403(R) (2005).

²¹R. C. Bourret, Nuovo Cimento **26**, 1 (1962).